Chemical ozone loss and chlorine activation in the Antarctic winters 2013–2020

R. Roy[1,2*], P. Kumar[1], J. Kuttippurath[1*], F. Lefevre[3]

[1] CORAL, Indian Institute of Technology Kharagpur, Kharagpur–721302, India.

[2] Department of Physical Oceanography, Cochin University of Science and Technology, Kochi, India.

[3] LATMOS/IPSL, Sorbonne Université, UVSQ, CNRS, Paris, France

Correspondence to: R. Roy and J. Kuttippurath (rainaroy2105@gmail.com; jayan@coral.iitkgp.ac.in)

Abstract

The annual formation of an ozone hole in the austral spring has regional and global climate implications. Antarctic ozone hole has already changed the precipitation, temperature and atmospheric circulation patterns, and thus, the surface climate of many regions in the Southern Hemisphere (SH). Therefore, the study of ozone loss variability is important to assess its consequential effects on the climate and public health. Our study uses satellite observations from the Microwave Limb Sounder on Aura and the passive tracer method to quantify the ozone loss for the past eight years (2013–2020) in the Antarctic. We observe the highest ozone loss (about 3.5 ppmv) in 2020, owing to the high chlorine activation (about 2.2 ppbv), steady polar vortex, and huge expanses of polar stratospheric clouds (PSCs) (12.6 million km^2) in the winter. The spring of 2019 also showed a high ozone loss, although the year had a rare minor warming in mid-September. The chlorine activation in 2015 (1.9 ppbv) was the weakest, and the wave forcing from the lower latitudes was very high in 2017 (up to -60 Kms^{-1}). The analysis shows significant interannual variability in the Antarctic ozone as compared to the immediate previous decade (2000–2010). The study helps to understand the role of dynamics and chemistry in the interannual variability of ozone depletion over the years.

Keywords: Antarctic; Ozone loss estimates; Polar Vortex; Climate Change; Model simulations

Short title: Antarctic ozone loss in 2013–2020

Introduction

An important event in the Antarctic stratosphere during the austral spring that has caught global attention ever since its discovery in the 1980s is the Antarctic ozone hole (Farman et al., 1985). The chlorine free radicals released from the chlorofluorocarbons (CFCs) and other ozone-depleting substances (ODSs) activate the catalytic cycles that lead to severe ozone loss (e.g., Stolarski and Cicerone, 1974; Rowland et al., 1976). The extreme cold conditions that prevail in the poles facilitate the formation of Polar Stratospheric Clouds (PSCs), which serve as the activation surface for the ODSs. Apart from these, the relatively stable Antarctic polar vortex also contributes significantly to the annual formation of ozone holes (Solomon et al., 2014). Since the discovery of ODSs in the 1970s from anthropogenic activities, ozone loss has continued to rise and reached its worst phase in the late 1980s and early 1990s (e.g., WMO, 2014). The increase in ODSs was curtailed after the enactment of the Montreal Protocol in 1987. Ratifying the environmental treaty led to a stabilisation of ozone loss from the late 1990s to the early 2000s in the Antarctic. Despite this, there was no significant increase in total column ozone (TCO) during those times (e.g., Weatherhead et al., 2000; WMO, 2007; Angell et al., 2009). Beyond 2000, significant recovery trends in the lower stratospheric ozone were presented with evidence from both ground and satellite observations (e.g., Yang et al., 2008; Salby et al., 2011; Solomon et al., 2016; Chipperfield et al., 2017; Kuttippurath and Nair, 2017; de Laat et al., 2017; Pazmiño et al., 2018; Wespes et al., 2019; Johnson et al., 2023). A reduction in the saturation of ozone loss over the period 2001–2017 is also observed in the Antarctic, confirming the positive ozone trends in the region (Kuttippurath et al., 2018). There are also studies showing the changes in surface climate of Southern Hemisphere (SH) due to ozone hole, by altering its temperature, winds, general circulation and precipitation. Therefore, understanding of the Antarctic ozone variability is important for assessing the future changes in the climate of SH (e.g., Gillett and Thompson, 2003; Polvani et al., 2011). For instance, the modelling studies of Kang et al. (2013) and Brönnimann et al. (2017) show increased extreme precipitation in the austral summer in the southern high and subtropical latitudes, and enhanced precipitation in the southern flank of South Pacific Convergence Zone, respectively, due to the Antarctic ozone hole.

Here, we present the long-term analysis of ozone loss for the period 2013–2020 considering the chemical and dynamical characteristics of the winters. Although a few of the years have been studied individually, the long-term analysis helps in better understanding the evolution of the winters (e.g., WMO, 2015; Krummel et al., 2016; Wargan et al., 2020; Manney et al., 2020; Klekociuk et al., 2021). The dynamics of these winters are studied using different meteorological parameters. The study offers a high-resolution analysis of the interannual variability of

ozone at various altitudes using the data obtained from the Aura Microwave Limb Sounder (MLS) (Froidevaux et al., 2008; Santee et al., 2008). The ozone loss is calculated using the passive tracer simulated by the REPROBUS (Reactive Processes Ruling the Ozone Budget in the Stratosphere) chemical transport model (CTM) (Lefèvre et al., 1994). Therefore, we use a single dataset and the same method to estimate ozone loss for all eight years to assess the interannual variability, which would make the comparisons among the winters meaningful, coherent and robust.

Data and Methods

We have analysed the meteorology of the winters 2013–2020 using the Modern-Era Retrospective Analysis for Research and Applications (MERRA-2) data (Gelaro et al., 2017) as these data include the information regarding all weather parameters such as temperature and winds, planetary waves, heat flux and polar stratospheric clouds (PSCs). MERRA 2 data are available for 42 pressure levels at a spatial resolution of 0.5° x 0.625°. The nature of austral springs is studied by the polar cap temperature zonally averaged between 60° and 90° S at 100 hPa, the minimum polar cap temperature at 10 hPa, the area of PSCs at 460 K, and the mean heat flux averaged over the latitude band 45°–75° S. The PSC area is estimated using the amount of water vapour of 5 ppm and nitric acid of 4.97 ppt at 460 K. Further details are provided on https://ozonewatch.gsfc.nasa.gov/meteorology/temp_2022_MERRA2_SH.html). Besides, the MERRA 2 dataset is also employed to analyse the vertical evolution of temperature averaged over 60°–90° S.

The ozone loss is estimated using the passive tracer method (e.g. Kuttippurath et al., 2015). The tracer is simulated by the REPROBUS CTM, which is identical to ozone, but without interactive chemistry. It is a three-dimensional model driven by the European Centre for Medium-Range Weather Forecasts (ECMWF) operational analyses. The analysis is performed for the altitude range of 1000–0.01 hPa (137 levels). In the model, the advection is performed by the winds on the hybrid sigma-pressure coordinates, and the trace gases are advected by a semi-lagrangian technique (Williamson and Rasch, 1989). In our study, the passive tracer is initialised on 1st of June each year and continued until the end of November. The loss is then computed by subtracting the measured ozone from the modelled passive ozone, which is also called inferred ozone loss. Note that the model simulations are used only for the passive ozone in this study. Since the tracer initialisation was made on 1st of April in 2020, there was a consequential offset in its values with respect to other years on 1st of June. This offset is corrected for the ozone loss computation for that year. The loss in each day is estimated inside the polar vortex as it is more prevalent there, and the vortex edge is calculated using the equivalent latitude (Nash et al., 1996; Müller et al., 2005). The measurements of ozone and chlorine monoxide (ClO) are taken from the MLS version 4.2. These ozone data have

90   a vertical resolution of 2–3 km, a vertical range of 261–0.02 hPa and an accuracy of 0.1–0.4 ppmv. The ClO

91   measurements are performed at 640 GHz, and these data have a vertical resolution of 3–3.5 km at 147–1 hPa with

92   an accuracy of about 0.2–0.4 ppbv. These ClO measurements have a latitude-dependent bias of around 0.2–0.4

93   ppbv, depending on the altitude (Livesey et al., 2013).

Results and Discussion

Meteorology of the winters

97   Fig. 1 shows the meteorology of the winters as illustrated with the polar cap temperature (60–90° S) at 100 hPa,

98   the minimum temperature averaged over 50°–90° S at 100 hPa, PSC area at 460 K and the heat flux averaged

99   between 45° and 75° S at 100 hPa. The top panel shows the mean temperature (60°–90° S) at 100 hPa, and the

100   coloured lines represent individual years. Temperature decreases from the beginning of winter (June) onwards and

101   reaches its lowest in August. The lowest temperature for most years is observed in August, but it continued to

102   September in 2015 and 2020. Temperature is in the order of 195–208 K during this period in most years (Fig. 1).

103   In the years 2013, 2014, 2015 and 2020, the temperature shows below 195 K (the PSC formation threshold).

104   However, the temperature shows a sudden rise from late August (202 K) to mid-September (218 K) in 2019,

105   indicative of the occurrence of a Sudden Stratospheric Warming (SSW). This event has been reported in some of

106   the previous studies and has been described as a minor Warming (mW) (e.g., Shen et al., 2020a,b; Yamazaki et al.,

107   2020; Roy et al., 2022). Temperature in August 2017 is also higher than that in previous years but lower than in

108   2019. There is a rise in temperature at the beginning of the austral spring. However, temperatures persist below

109   195 K during early September 2015. The lowest temperatures during the winter–spring period are found in 2015

110   and 2020, as depicted in Fig. 1.

111   Fig. 1 (second panel from top) shows the minimum polar cap temperature for each winter, and is lower than the

112   PSC formation threshold (195 K). This continues in the early spring for all years except in 2019, and the minimum

113   value rises soon after and is higher than 195 K in the late spring. The minimum temperature reaches this threshold

114   for most days and thus, the ideal conditions for the formation of PSCs are found in all winters. Therefore, the PSC

115   area has grown since the beginning of winter and is highest in August (up to 28 million km^2). Corresponding to the

116   periods of longest duration of minimum temperature, PSCs persist until early November in 2015, 2018 and 2020,

117   but are relatively short-lived in 2017 and 2019. As the mean temperature peaks in early to mid-September 2019,

118   the PSC area drops and diminishes by late September. However, the PSCs dissipated by mid-October in 2017.

4

A major factor affecting the strength of polar vortex is tropospheric forcing. Strength of this forcing is very weak in the Antarctic, except for a few winters. According to Zuev et al. (2019), the strengthening of Antarctic polar vortex in winter and spring is due to the seasonal temperature variations in the subtropical lower stratosphere. Fig. 1 (bottom) shows the tropospheric forcing estimated for all years. The heat flux averaged between the adjacent mid-latitudes and higher latitudes is directed southward, particularly in the late winter and early spring. The years 2019 and 2017 are characterised by very strong wave forcing, as shown by the high flux values (from -40 to -50 Kms^{-1}). Klekociuk et al. (2020) reported that the easterly phase of QBO favoured the enhanced wave activity in 2017; a reason for the relatively higher temperature in that winter. Milinevsky et al. (2019) and Evtushevsky et al. (2020) also found similar results for both winters. The zonal average of heat flux stays between -30 and 10 Kms^{-1} for most winters, and the flux increases as the spring approaches. However, these forcings are weak in the years 2015 and 2020.

Temporal evolution of temperature with altitude

Fig. 2 shows the temporal evolution of zonal mean (60°–90° S) temperature profiles in the Antarctic for the years 2013–2020. The coloured contours show the temperature across the seasons and white contour lines represent 188, 195 and 210 K. Here, the zonal winds (westerlies) are overlaid with black contours, and the easterlies are in red. In general, temperature increases towards the end of spring in the stratosphere, but it started to rise in the lower stratosphere much earlier during the spring of 2019 and 2017. Temperature contours of 250–265 K extend to slightly below 10 hPa and there is a small reduction in the speed of westerlies during the period. Temperatures below 195 K are found in the lower stratosphere (100–70 hPa) until mid-October in 2015 and 2020. Similarly, the area covered by < 195 K was also moderately large in 2013, 2014, 2016 and 2018. However, this is lowest in 2019 and relatively very small in 2017. The appearance of easterlies below 10 hPa is late (end of November) and thus, the vortex lasted longer in 2015 and 2020, whereas as early as late October in 2017 and 2019. We also made an assessment inside the vortex, to examine the consistency of our analysis with and without the vortex criterion (see Figure S1). The key features are same in both analyses, such as the very low temperatures in the lower stratosphere, strong westerlies and late appearance of easterlies in the middle stratosphere in 2015 and 2020, the early appearance of easterlies and the minor warming in 2019, and the large and extended period of PSC threshold temperature (195 K) in 2018. Since the meteorology is different inside the vortex, small differences in the temperature (e.g., PSC threshold area) and wind (middle stratospheric westerlies in 2015 and 2020) values are also found between the two.

Ozone, chlorine activation and ozone loss

Fig. 3 shows the temporal evolution of ozone (in ppmv) inside the vortex deduced from the MLS data for the period 2013–2020. The ozone is lost in the lower altitudes as time progresses in spring, as illustrated in Fig. 3. It is observed from previous studies that the ozone loss is maximum in the lower stratosphere in all years (Solomon et al., 1999). Contrary to this, ozone increases in the upper stratosphere as the winter progresses towards spring. Ozone in the lower stratosphere (400–600 K) is around 0.1–3 ppmv in 2013, 2014, 2015, 2016, 2018 and 2020. Unlike in the cold winters, ozone is slightly higher (by 0.5–1.5 ppmv) in the lowermost stratosphere in 2019. Similarly, in 2017, ozone in the lower stratosphere (400–450 K) is higher than that in the previous cold years, owing to the higher temperature there. The lowest ozone for the altitude range of 400–475 K is observed in 2015, 2018 and 2020, in which the 0.5 ppmv contour extends to 475–500 K.

Figure 4 presents the temporal evolution of ClO (right) and ozone loss (left) at different altitudes during the period of study. Since there are unreasonably high tracer values in June due to initialisation problem, the ozone loss is not calculated up to 10 June 2018 and 20 July 2019. In general, ozone loss is highest at 400–550 K (lower stratosphere) during September and October in all years. The loss is smaller than 1.4 ppmv in the upper stratosphere, mostly driven by the NO_x-based chemistry (e.g., Kuttippurath et al., 2015). The loss in 2014 and 2015 is almost similar, about 2.6–3.0 ppmv at the peak ozone loss altitude (450–550 K) during September and October. The loss in 2013 reaches up to 3.0 ppmv by mid-October and is higher than in 2014, 2015, 2017 and 2018 (e.g., Vargin et al., 2020). The ozone loss reported by Strahan et al. (2018) for 2015 is similar to the very cold winters in Antarctica and is slightly higher than our estimate for that winter. The ozone loss with altitude is larger in 2015 than other winters (see Fig. 4). The preconditioning for ozone loss in 2013 and 2014 was ensured by high chlorine activation at the same altitude range (Kuttippurath et al., 2015). Among these three years (2013–2015), before the period of highest ozone loss, chlorine activation reaches its peak in August and September. ClO amounts up to 2.2 ppbv in 2013 and 2014, and 2.0 ppbv in 2015 during this period. This high chlorine activation lasted for almost a month at the peak ozone loss altitudes (450–550 K) in 2013, but for a relatively shorter period in 2014 and 2015. Similar values for ozone loss and ClO (1.8–2.2 ppbv) are also estimated for 2017 and 2018, and the highest ClO stayed intact for 15–20 days before attaining the maximum ozone loss.

The ozone loss in 2016 is about 3–3.2 ppmv in September and 3.4 ppmv in October. Note that the ozone hole, PSC occurrence and chlorine activation (more than a month, up to 2.2 ppbv) lasted longer in this year. An extensive

ozone hole from late August to mid-November is found in 2019. However, ozone increased after the minor warming, and thus the ozone hole size (Fig. 3) and ozone loss reduced significantly thereafter (Fig. 4). The chlorine activation was very strong and continuous from August to September (above 2.2 ppbv) in this year. Despite the minor warming, the ozone loss in 2019 (3.0–3.4 ppmv) is similar to that in 2016. The nature of spring 2019 was similar to the previous warm Antarctic years of 1988 and 2002, as the vortex was short-lived and highly variable due to strong tropospheric forcing and SSW (Manney et al., 2020; Klekociuk et al., 2021). The peak ozone loss in 2019 is about 3.4 ppmv, which is higher than that in other winters, except 2020 (Wargan et al., 2020; Roy et al., 2022). The chlorine activation remained at its peak value (2.0–2.2 ppbv) for several days in August before reaching the peak ozone loss in 2019, and the spatial distribution (450–550 K) of these high ClO values is the largest compared to all other years. The 2020 ozone loss is very high (up to 3.6 ppmv) and exceeds the maximum ozone loss of other winters. The chlorine activation rose in the early spring (September) (2.0–2.2 ppbv) and is similar to that in 2016. The high values of ozone loss may have resulted from the increased aerosol loading from the Australian bushfires in 2020 (e.g., Stone et al., 2021). A recent study by Ansmann et al. (2022) shows that about 10–20% of the ozone loss in 2020 was driven by the wildfire smoke that caused the growth of PSC particles.

Interannual variability of ozone loss

The interannual variability of ozone loss, PSC and chlorine activation is shown in Fig. 5. Here, the ozone loss is computed by taking the average of ozone loss from day 270 to 300 (the peak loss period) in the altitude range 450–550 K (the peak loss altitudes, see Fig. 4). Similarly, the chlorine activation is indicated as the average of ClO over the same altitude range, but for the days between 210 and 270 (peak chlorine activation period). The weighted mean of PSC area is shown with black solid line for the years 2013–2020. Note that the peak ozone loss duration and altitude range are different in different winters (e.g. 2018 and 2020). The smallest ozone loss is estimated for the years 2015 and 2017 because of relatively weak chlorine activation in those winters. The mean ozone loss is about 2.4 ppmv and ClO is about 1.75–1.95 ppbv in both years. However, the PSC area in 2015 (11.9 million km^2) was higher than most of other cold winters. The larger PSC area is mostly because of the lower temperature conditions that lasted longer in the winter. Tully et al. (2019) identified 2015 as one of the most severe and extreme winters, as also observed in our study. The PSC area in 2017 (10.2 million km^2) is smaller and therefore, ozone loss is lower as compared to that in 2015, which is consistent with the results of Braathen (2018).

The highest ozone loss is estimated in 2020 (3.1 ppmv) in the spring, which is followed by 2016 (3.0 ppmv). The chlorine activation for both years is also higher than that of a few other cold winters, as shown by the ClO values of about 2.1–2.2 ppbv. The highest ozone loss in 2020 is favoured by the very large PSC area (12.6 million km^2). The 2018 spring was also unique in comparison to the other years as a consequence of the high chlorine activation (2.2 ppbv) and very large PSC area (12.0 million km^2). The chlorine activation was very high in 2019 (2.1 ppbv), but the relatively lower ozone loss during this particular period is a direct consequence of its unfavourable dynamic condition (SSW). The PSC area is also lowest in 2019 (9.4 million km^2) among the winters due to SSW. The ozone loss (2.7–2.8 ppmv) and chlorine activation (2.1–2.2 ppbv) are similar in other winters.

Table 1 shows the partial column ozone loss estimated with the MLS data and REPROBUS passive ozone simulations for two different altitude ranges. The partial column loss at 350–750 K yields similar values for most winters, as the highest loss is estimated for 2015, 2016, 2018 and 2019 (around 163±16 DU), consistent with the meteorology of the winters. However, the lowest column loss (128±12 DU) is estimated for the winter 2020, as the vertical spread of ozone loss is limited beyond the peak ozone loss altitude range of 450–550 K in this winter (see Fig. 4). Similarly, ozone loss in the moderately cold winters shows a loss of about 154±15 DU (2013 and 2014), but very small loss in 2017 (134±13 DU). The column loss computed at 400–600 K, the highest ozone loss altitudes in the Antarctic, has slightly lower values as expected. In general, there is an average difference of about 40 DU (higher than the 400–600 K) ozone loss between these altitude ranges (e.g., Kuttippurath et al., 2015). The loss is highest in 2019 (145±14 DU) at 400–600 K as in the case of 350–750 K, but smallest in 2015 (107±10 DU). This suggests that there is higher ozone loss at altitudes above 600 K in the very cold winter of 2015 (see Fig. 4). On the other hand, ozone loss and its difference between these two altitude ranges are very small for 2020 and 2017, as discussed before.

Conclusions

We analyse the ozone loss for the past 8 years (2013–2020) in the Antarctic. The year 2019 had a warm winter with a mW in mid-September. The winter of 2017 also shows similar characteristics, such as the sudden increase in temperature during late August, higher minimum temperature (about 205 K) in August than in other years and the sharp decrease in PSC area towards the end of September. The heat flux magnitude for the year (2017) is also higher than that in other winters (up to -60 Kms^{-1}), suggesting that it was a disturbed warm winter. We find a minimal ozone loss in 2017 and it stayed less than 2.8 ppmv (110±11 DU at 400–600 K) for most of October and

September. Chlorine activation was also below 1.8 ppbv during August and September in the year. Conversely, the wave fluxes are lowest in 2015. The temperature and PSC area follow similar temporal evolution in 2013, 2014, 2015, 2016 and 2018. Winter 2020 exhibits unique meteorology with a long-lasting occurrence of vortex-wide PSCs (12.6 million km^2) and thus, shows the highest ozone loss (3.5 ppmv). On the other hand, the lowest ozone loss (2.5 ppmv or 107±10 DU at 400–600 K) is estimated in 2015. Our study, thus, helps in understanding how the chlorine activation and meteorology of the winters influence the variability of ozone. Dynamics and chemistry of the winters play their respective roles in the ozone loss process. The winter of 2019 is an example of favourable chemistry helping in large loss in ozone, though the dynamical conditions were unfavourable.

Acknowledgements

Data availability

The data used in this study are publicly available. The MLS data are available from https://disc.gsfc.nasa.gov/. The meteorological data are acquired through https://ozonewatch.gsfc.nasa.gov. The REPROBUS data are acquired through IPSL, http://cds-espri.ipsl.fr/. The analysed data/codes can also be provided on request.

Competing Interests

JK is an Editor of Atmospheric Chemistry and Physics. Otherwise, no competing interests.

Author Contributions

JK conceived the idea, and JK and RR wrote the original manuscript. The manuscript was subsequently revised with inputs from PK and FL. The model runs and model results were analyzed by FL. The data analyses and figures made by RR and PK. All authors participated in discussions and made suggestions, which were considered for the final draft.

266 **Table 1:** The partial column ozone loss computed using the MLS ozone measurements and modelled tracer by
267 applying the passive method. The column loss is estimated for the peak ozone altitude ranges of 350–750 K and
268 400–600 K. The ozone column loss estimates have an uncertainty of about 10%.

| Year	Ozone column loss 350−750 K (DU)	Ozone column Loss 400−600 K (DU)
2013	153	122
2014	156	122
2015	169	107
2016	163	128
2017	134	110
2018	165	115
2019	169	145
2020	128	120

269
270
271
272
273
274
275
276
277
278
279
280
281
282
283
284
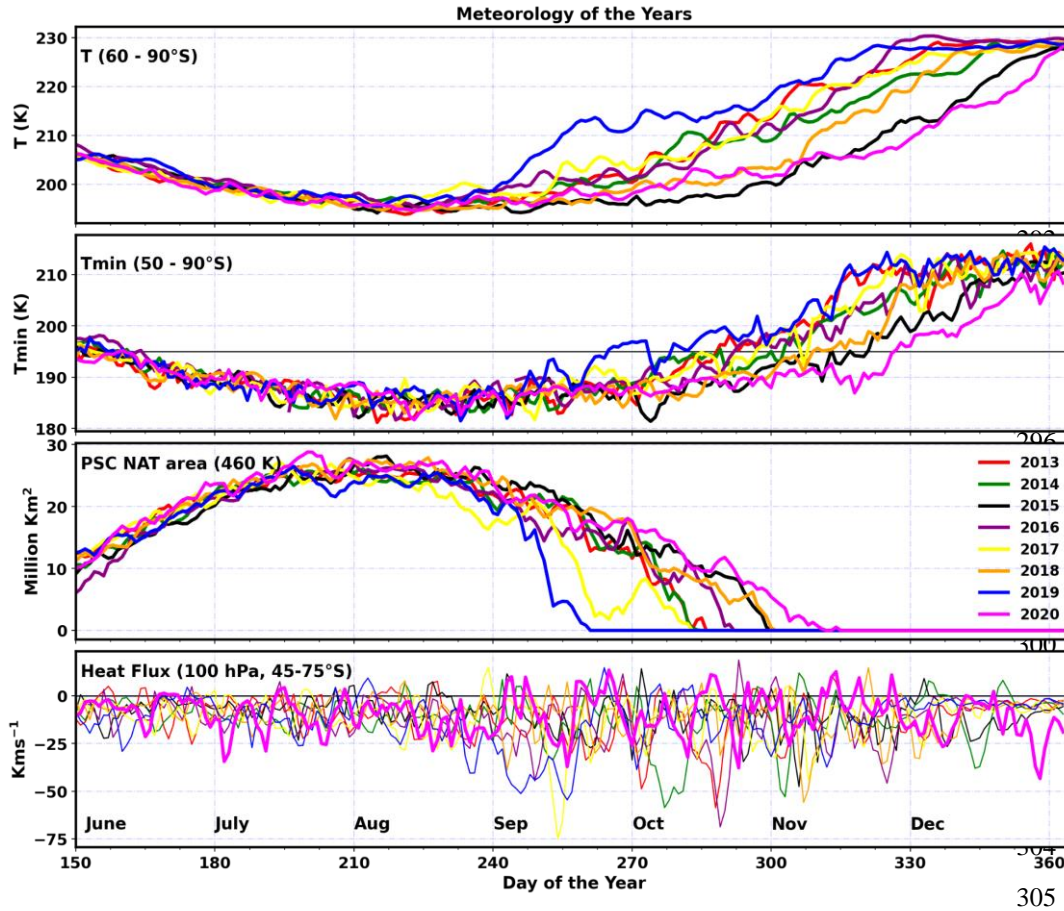
285
286

Figure 1: Meteorology of the years (2013–2020). Top panel shows the zonal average temperature (60°–90° S) at 100 hPa. Second panel (from top) shows the minimum temperature at 100 hPa. The black horizontal line in the panels shows 195 K (PSC formation threshold). Third panel (from top) shows the PSC area at 460 K and the bottom panel shows the mean heat flux (45°–75° S) at 100 hPa. The black horizontal line in the bottom panel shows zero heat flux.
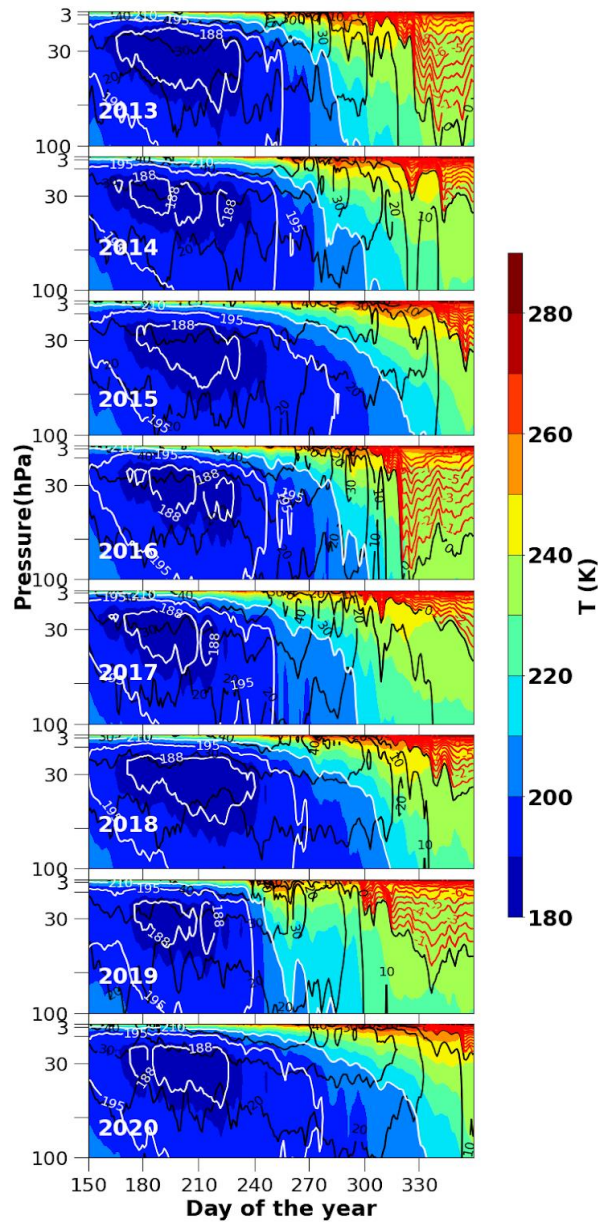
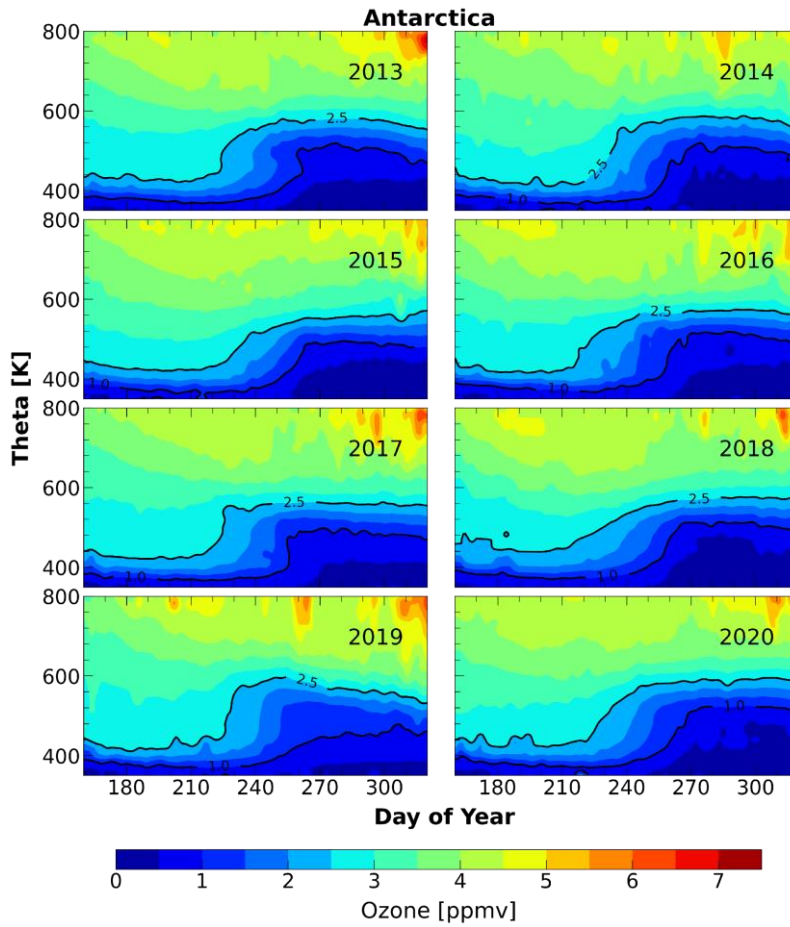**Figure 2:** Seasonal march of the zonal mean temperature for the period 2003–2020 averaged over the latitudes 60°–90° S. The contours show the temperature and white contours represent specific temperatures such as 188, 195 and 210 K. The zonal wind velocities are overlaid. The black contour lines show the westerlies and the red contour lines show the easterlies.

12

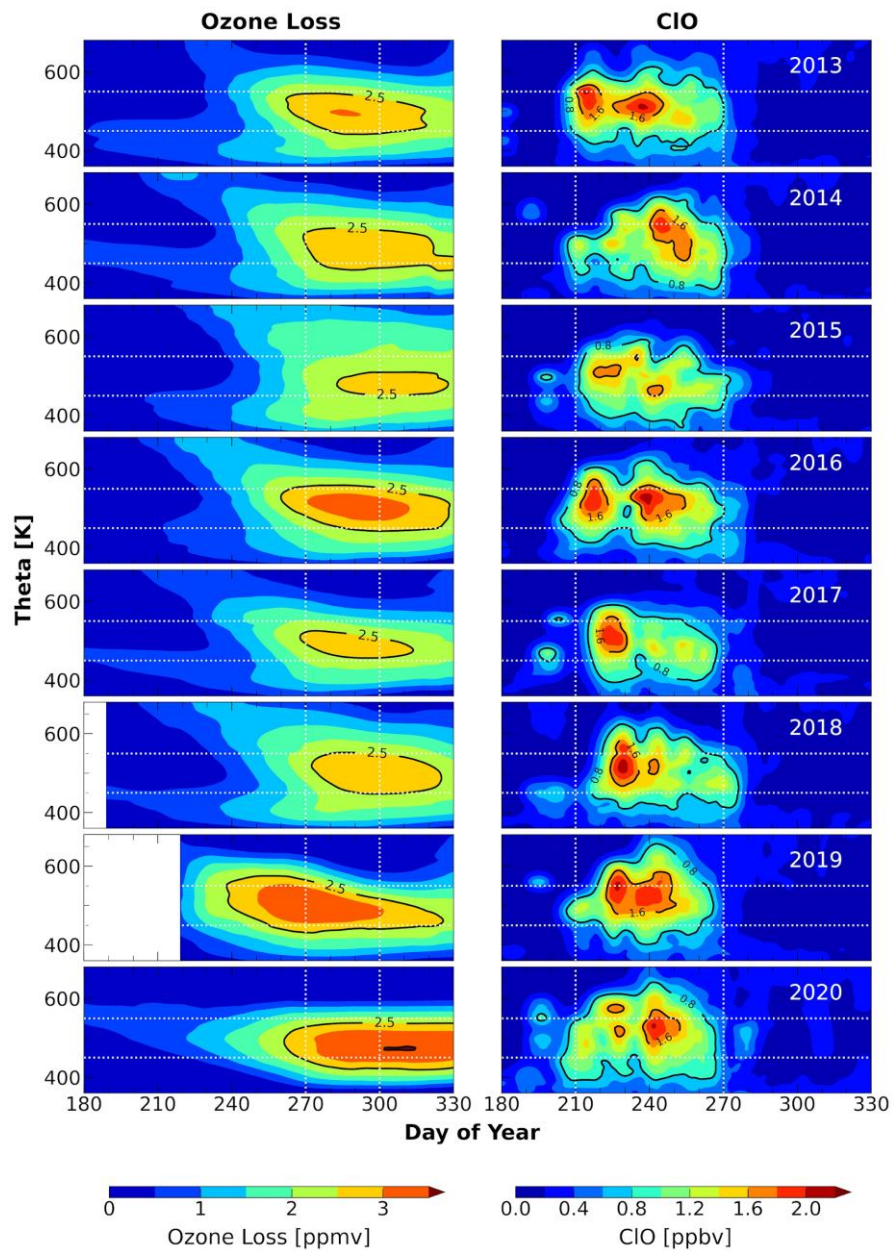**Figure 3:** Temporal evolution of the vertical profiles of ozone averaged inside the vortex for the winters 2013–2020 in the Antarctic. The temporal evolution is analysed using the MLS ozone data at 350–800 K for the period June–November. The black contours represent 1.0 and 2.5 ppm of ozone.

**Figure 4:** Temporal evolution of ozone loss estimated from MLS measurements using REPROBUS passive tracer (left). The MLS ClO measurements for the altitude range 350–700 K for the period 2013–2020 (right). The ozone loss estimates and ClO measurements are selected inside the polar vortex as per the Nash et al. (1996) criterion. Ozone loss is not computed up to 10th June in 2018 and 20th July in 2019 because of the unavailability of tracer values. The black contours represent 2.5 and 3.5 ppm of ozone loss (left panel) and 0.8 and 1.6 ppb of ClO (right panel).

14

343

344

345
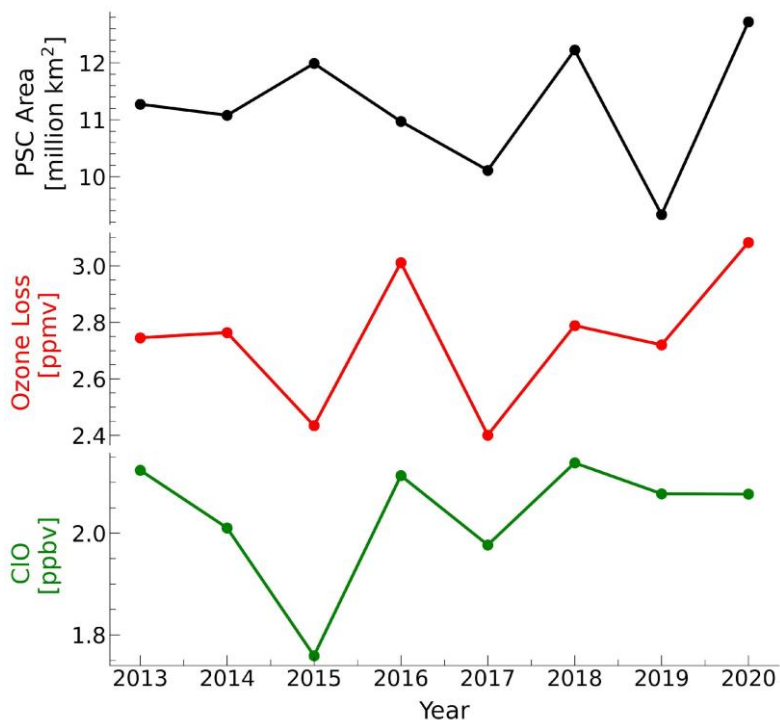
Figure 5: The vortex-averaged ozone loss estimated from the MLS measurements using the passive method, peak ClO measurements, and the weighted average of area of PSC for the period 2013–2020. The mean ozone loss is estimated over the altitude range 450–550 K and between day 270 and 300 (maximum ozone loss days). The ClO measurements are averaged over the altitude range 450–550 K and between day 210 and 270; representing the strong chlorine activation period and altitudes.

351

352

353

354

References

Angell, J. K. and Free, M.: Ground-based observations of the slowdown in ozone decline and onset of ozone increase, J. Geophys. Res., 114, D07303, doi:10.1029/2008JD010860, 2009.

Ansmann, A., Ohneiser, K., Chudnovsky, A., Knopf, D. A., Eloranta, E. W., Villanueva, D., Seifert, P., Radenz, M., Barja, B., Zamorano, F., Jimenez, C., Engelmann, R., Baars, H., Griesche, H., Hofer, J., Althausen, D., and Wandinger, U.: Ozone depletion in the Arctic and Antarctic stratosphere induced by wildfire smoke, Atmos. Chem. Phys., 22, 11701–11726, doi:10.5194/acp-22-11701-2022, 2022.

Bandoro, J., Solomon, S., Donohoe, A., Thompson, D.W.J., and Santer, B.D.: Influences of the Antarctic ozone hole on Southern Hemispheric summer climate change, J. Climate, 27(16), 6245–6264, doi: 10.1175/JCLI-D-13-00698.1, 2014.

Braathen, G. O.: Observations of the Antarctic Ozone Hole from 2003 to 2017, p. 16503, 2018.

Brönnimann, S., Coper, J.M.*, Rozanov, E., Fischer, A.M.*, Morgenstern, O., Zeng, G., Akiyoshi, H., & Yamashita, Y.: Tropical circulation and precipitation response to ozone depletion and recovery. Environmental Research Letters, 12 (6), https://doi.org/10.1088/1748-9326/aa7416, 2017.

Butler, A., Daniel, J. S., Portmann, R. W., Ravishankara, A., Young, P. J., Fahey, D. W., and Rosenlof, K. H.: Diverse policy implications for future ozone and surface UV in a changing climate, Environ. Res. Lett., 11, 064017, doi:10.1088/1748-9326/11/6/064017, 2016.

Chipperfield, M. P., Bekki, S., Dhomse, S., Harris, N. R., Hassler, B., Hossaini, R., Steinbrecht, W., Thiéblemont, R., and Weber, M.: Detecting recovery of the stratospheric ozone layer, Nature, 549, 211, doi:10.1038/nature23681, 2017.

de Laat, A. T. J., van Weele, M., and van der A, R. J.: Onset of stratospheric ozone recovery in the Antarctic ozone hole in assimilated daily total ozone columns, J. Geophys. Res.-Atmos., 122, 11880–11899, doi:10.1002/2016JD025723, 2017.

Evtushevsky, O. M., Klekociuk, A. R., Kravchenko, V. O., Milinevsky, G. P., and Grytsai, A. V.: The influence of large amplitude planetary waves on the Antarctic ozone hole of austral spring 2017, J. South. Hemisph. Earth Syst. Sci., 69, 57–64, doi:10.1071/ES19022, 2019.

Farman, J. C., Gardiner, B. G., and Shanklin, J. D.: Large losses of total ozone in Antarctica reveal seasonal C1Ox/NOx interaction, Nature, 315, 207-210, 1985.

16

Froidevaux, L., Jiang, Y. B., Lambert, A., Livesey, N. J., Read, W. G., Waters, J. W., Browell, E. V., Hair, J. W., Avery, M. A., McGee, T. J., Twigg, L. W., Sumnicht, G. K., Jucks, K. W., Margitan, J. J., Sen, B., Stachnik, R. A., Toon, G. C., Bernath, P. F., Boone, C. D., Walker, K. A., Filipiak, M. J., Harwood, R. S., Fuller, R. A., Manney, G. L., Schwartz, M. J., Daffer, W. H., Drouin, B. J., Cofield, R. E., Cuddy, D. T., Jarnot, R. F., Knosp, B. W., Perun, V. S., Snyder, W. V., Stek, P. C., Thurstans, R. P., and Wagner, P. A.: Validation of Aura Microwave Limb Sounder stratospheric ozone measurements, J. Geophys. Res., 113, 15-20, https://doi.org/10.1029/2007JD008771, 2008.

Gelaro, R., McCarty, W., Suárez, M. J., Todling, R., Molod, A., Takacs, L., Randles, C. A., Darmenov, A., Bosilovich, M. G., Reichle, R., Wargan, K., Coy, L., Cullather, R., Draper, C., Akella, S., Buchard, V., Conaty, A., da Silva, A. M., Gu, W., Kim, G.-K., Koster, R., Lucchesi, R., Merkova, D., Nielsen, J. E., Partyka, G., Pawson, S., Putman, W., Rienecker, M., Schubert, S. D., Sienkiewicz, M., and Zhao, B.: The Modern-Era Retrospective Analysis for Research and Applications, Version 2 (MERRA-2), J. Climate, 30, 5419–5454, https://doi.org/10.1175/JCLI-D-16-0758.1, 2017.

Gillett, N. P., Thompson, D. W.: Simulation of recent southern hemisphere climate change, Science (New York, N.Y.), 302(5643), 273–275, https://doi.org/10.1126/science.1087440, 2003.

Johnson, B. J., Cullis, P., Booth, J., Petropavlovskikh, I., McConville, G., Hassler, B., Morris, G. A., Sterling, C., and Oltmans, S.: South Pole Station ozonesondes: variability and trends in the springtime Antarctic ozone hole 1986–2021, Atmos. Chem. Phys., 23, 3133–3146, https://doi.org/10.5194/acp-23-3133-2023, 2023.

Kang, S. M., Polvani, L. M., Fyfe, J. C., Son, S.-W., Sigmond, M., Correa, G. J. P.: Modeling evidence that ozone depletion has impacted extreme precipitation in the austral summer, Geophys. Res. Lett., 40, 4054–4059, doi:10.1002/grl.50769, 2013.

Klekociuk, A., Tully, M. B., Krummel, P. B., Evtushevsky, O., Kravchenko, V., Henderson, S. I., et al.: The Antarctic ozone hole during 2017, University Of Tasmania, Journal contribution, https://hdl.handle.net/102.100.100/558640, 2020.

Klekociuk, A. R., Tully, M. B., Krummel, P. B., Henderson, S. I., Smale, D., Querel, R., Nichol, S., Alexander, S. P., Fraser, P. J., and Nedoluha, G.: The Antarctic ozone hole during 2018 and 2019, J. South. Hemisphere Earth Syst. Sci., 71, 66–91, doi:10.1071/ES20010, 2021.

Krummel, P. B., Fraser, P. J., and Derek, N.: The 2015 Antarctic ozone hole and ozone science summary: final report, CSIRO: Australia, iv, 27 pp, 2016.

Kuttippurath, J., Kumar, P., Nair, P. J., and Pandey, P. C.: Emergence of ozone recovery evidenced by reduction in the occurrence of Antarctic ozone loss saturation, Npj Climate and Atmospheric Science, 1(1), doi:10.1038/s41612-018-0052-6, 2018.

Kuttippurath, J., and Nair, P. J.: The signs of Antarctic ozone hole recovery, Sci. Rep., 7, 585, doi:10.1038/s41598-017-00722-7, 2017.

Kuttippurath, J., Godin-Beekmann, S., Lefèvre, F., Santee, M. L., Froidevaux, L., and Hauchecorne, A.: Variability in Antarctic ozone loss in the last decade (2004–2013): high-resolution simulations compared to Aura MLS observations, Atmos. Chem. Phys., 15, 10385–10397, https://doi.org/10.5194/acp-15-10385-2015, 2015.

Langematz, U., and Kunze, M.: An update on dynamical changes in the Arctic and Antarctic stratospheric polar vortices, Clim Dyn, 27, 647–660, https://doi.org/10.1007/s00382-006-0156-2, 2006.

Lefèvre, F., Brasseur, G. P., Folkins, I., Smith, A. K., and Simon, P.: Chemistry of the 1991/1992 stratospheric winter: three-dimensional model simulations, J. Geophys. Res., 99, 8183–8195, 1994.

Livesey, N. J., Read, W. G., Froidevaux, L., Lambert, A., Manney, G. L., Pumphrey, H. C., Santee, M. L., Schwartz, M. J., Wang, S., Cofeld, R. E., Cuddy, D. T., Fuller, R. A., Jarnot, R. F., Jiang, J. H., Knosp, B. W., Stek, P. C., Wagner, P. A., and Wu, D. L.: Earth Observing System (EOS) Aura Microwave Limb Sounder (MLS) Version 3.3 and 3.4 Level 2 data quality and description document, JPL D-33509, Propulsion Laboratory, California Institute of Technology, Pasadena, California, USA, 1–164, 2013.

Manney, G. L., Livesey, N. J., Santee, M. L., Froidevaux, L., Lambert, A., Lawrence, Z. D., et al.: Record-low Arctic stratospheric ozone in 2020: MLS observations of chemical processes and comparisons with previous extreme winters, Geophys. Res. Lett., 47, e2020GL089063, https://doi.org/10.1029/2020GL089063, 2020.

Milinevsky, G., Evtushevsky, O., Klekociuk, A., Wang, Y., Grytsai, A., Shulga, V., Ivaniha, O.: Early indications of anomalous behaviour in the 2019 spring ozone hole over Antarctica, Int. J. Remote Sens., 41, 7530–7540, https://doi.org/10.1080/2150704X.2020.1763497, 2020.

Müller, R., Tilmes, S., Konopka, P., Grooß, J.-U., Jost, H.-J.: Impact of mixing and chemical change on ozone-tracer relations in the polar vortex, Atmos. Chem. Phys., 5, 3139–3151, https://doi.org/10.5194/acp-5-3139-2005, 2005.

Nash, E. R., Newman, P. A., Rosenfield, J. E., Schoeberl, M. R.: An objective determination of the polar vortex using Ertel's potential vorticity, J. Geophys. Res., 101, 9471–9478, 1996.

Pazmiño, A., Godin-Beekmann, S., Hauchecorne, A., Claud, C., Khaykin, S., Goutail, F., Wolfram, E., Salvador, J., Quel, E.: Multiple symptoms of total ozone recovery inside the Antarctic vortex during austral spring, Atmos. Chem. Phys., 18, 7557-7572, https://doi.org/10.5194/acp-18-7557-2018, 2018.

Polvani, L. M., Previdi, M., England, M. R., Chiodo, G., Smith, K. L.: Substantial twentieth-century Arctic warming caused by ozone-depleting substances, Nat. Clim. Chang., 10, 130–133, https://doi.org/10.1038/s41558-019-0677-4, 2020.

Polvani, L. M., Waugh, D. W., Correa, G. J. P., Son, S. -W.: Stratospheric ozone depletion: The main driver of twentieth-century atmospheric circulation changes in the Southern Hemisphere, J. Clim., 24(3), 795–812, 2011.

Rowland, F. S., Spencer, J. E., Molina, M. J.: Stratospheric formation and photolysis of chlorine nitrate, J. Phys. Chem., 80, 2711-2713, 1976.

Roy, R., Kuttippurath, J., Lefèvre, F., et al.: The sudden stratospheric warming and chemical ozone loss in the Antarctic winter 2019: comparison with the winters of 1988 and 2002, Theor. Appl. Climatol., 149, 119–130, https://doi.org/10.1007/s00704-022-04031-6, 2022.

Salby, M., Titova, E., Deschamps, L.: Rebound of Antarctic ozone, Geophys. Res. Lett., 38, L09702, https://doi.org/10.1029/2011GL047266, 2011.

Santee, M., MacKenzie, I. A., Manney, G., Chipperfield, M., Bernath, P. F., Walker, K. A., Boone, C. D., Froidevaux, L., Livesey, N., Waters, J. W.: A study of stratospheric chlorine partitioning based on new satellite measurements and modeling, J. Geophys. Res., 113, D12307, https://doi.org/10.1029/2007JD009057, 2008.

Shen, X., Wang, L., Osprey, S.: Tropospheric forcing of the 2019 Antarctic sudden stratospheric warming, Geophys. Res. Lett., 47, e2020GL089343, https://doi.org/10.1029/2020GL089343, 2020.

Shen, X., Wang, L., Osprey, S.: The Southern Hemisphere sudden stratospheric warming of September 2019, Sci. Bull., https://doi.org/10.1016/j.scib.2020.06.028, 2020.

Solomon, S., Ivy, D. J., Kinnison, D., Mills, M. J., Neely, R. R. III, Schmidt, A.: Emergence of healing in the Antarctic ozone layer, Science, 252, 269–274, https://doi.org/10.1126/science.aae006, 2016.

Solomon, S.: Stratospheric ozone depletion: A review of concepts and history, Rev. Geophys., 37, 275–316, https://doi.org/10.1029/1999RG900008, 1999.

Solomon, S., Haskins, J., Ivy, D. J., Min, F.: Fundamental differences between Arctic and Antarctic ozone depletion, Proc. Natl. Acad. Sci. U.S.A., 111, 6220–6225, https://doi.org/10.1073/PNAS.1319307111, 2014.

Stolarski, R. S., Cicerone, R. J.: Stratospheric chlorine: A possible sink for ozone, Can. J. Chem., 52, 1610-1615, 1974.

470 Stone, K. A., Solomon, S., Kinnison, D. E., Mills, M. J.: On Recent Large Antarctic Ozone Holes and Ozone
471 Recovery Metrics, Geophys. Res. Lett., 48, e2021GL095232, https://doi.org/10.1029/2021GL095232, 2021.

472 Strahan, S. E., Douglass, A. R.: Decline in Antarctic ozone depletion and lower stratospheric chlorine determined
473 from Aura Microwave Limb Sounder observations, Geophys. Res. Lett., 45, 382–390,
474 https://doi.org/10.1002/2017GL074830, 2018.

475 Tully, M. B., Klekociuk, A. R., Krummel, P. B., Gies, H. P., Alexander, S. P., Fraser, P. J., Henderson, S. I.,
476 Schofield, R., Shanklin, J. D., Stone, K. A.: The Antarctic ozone hole during 2015 and 2016, J. South.
477 Hemisphere Earth Syst. Sci., 69, 16, https://doi.org/10.1071/ES19021, 2019.

478 Vargin, P. N., Nikiforova, M. P., Zvyagintsev, A. M.: Variability of the Antarctic Ozone Anomaly in 2011–2018,
479 Russ. Meteorol. Hydrol., 45, 63–73, https://doi.org/10.3103/S1068373920020016, 2020.

480 Wargan, K., Weir, B., Manney, G. L., Cohn, S. E., Livesey, N. J.: The anomalous 2019 Antarctic ozone hole in
481 the GEOS constituent data assimilation system with MLS observations, J. Geophys. Res., 125, e2020JD033335,
482 https://doi.org/10.1029/2020JD033335, 2020.

483 Weatherhead, E. C., Reinsel, G. C., Tiao, G. C., Jackman, C. H., Bishop, L., Hollandsworth Frith, S. M., DeLuisi,
484 J., Keller, T., Oltmans, S. J., Fleming, E. L., Wuebbles, D. J., Kerr, J. B., Miller, A. J., Herman, J., McPeters, R.,
485 Nagatani, R. M., Frederick, J. E.: Detecting the recovery of total column ozone, J. Geophys. Res.-Atmos., 105,
486 22201–22210, https://doi.org/10.1029/2000JD900063, 2000.

487 Wespes, C., Hurtmans, D., Chabrillat, S., Ronsmans, G., Clerbaux, C., Coheur, P.-F.: Is the recovery of
488 stratospheric O3 speeding up in the Southern Hemisphere? An evaluation from the first IASI decadal record
489 (2008–2017), Atmos. Chem. Phys., 19, 14031–14056, https://doi.org/10.5194/acp-19-14031-2019, 2019.

490 Williamson, D. L., Rasch, P. J.: Two-dimensional semi-Lagrangian transport with shape-preserving interpolation,
491 Mon. Weather Rev., 117, 102–129, 1989.

492 WMO (World Meteorological Organization): Scientific Assessment of Ozone Depletion: 2006, Global Ozone
493 Research and Monitoring Project – Report No. 50, 572 pp., Geneva, 2007.

494 WMO (World Meteorological Organization): Scientific Assessment of Ozone Depletion: 2014, Global Ozone
495 Research and Monitoring Project Report, World Meteorological Organization, Geneva, Switzerland, 416 pp.,
496 2014.

497 World Meteorological Organization (WMO): WMO Antarctic Ozone Bulletins (2015), [Available online at
498 www.wmo.int/pages/prog/arep/WMOAntarcticOzoneBulletins2015.html], 2015.

499   Yamazaki, Y., Matthias, V., Miyoshi, Y., Stolle, C., Siddiqui, T., Kervalishvili, G., et al.: September 2019
500   Antarctic sudden stratospheric warming: Quasi-6-day wave burst and ionospheric effects, Geophys. Res. Lett.,
501   47, e2019GL086577, https://doi.org/10.1029/2019GL086577, 2020.

502   Yang, E.-S., Cunnold, D. M., Newchurch, M. J., Salawitch, R. J., McCormick, M. P., Russell, J. M., Zawodny, J.
503   M., Oltmans, S. J.: First stage of Antarctic ozone recovery, J. Geophys. Res., 113, D20308,
504   https://doi.org/10.1029/2007JD009675, 2008.

505   Zuev, V., Savelieva, E.: The cause of the strengthening of the Antarctic polar vortex during October–November
506   periods, J. Atmos. Solar-Terrestrial Phys., 190, https://doi.org/10.1016/j.jastp.2019.04.016, 2019.

507
508
509
510
511